nature microbiology

SUPPLEMENTARY INFORMATION

VOLUME: 2 | ARTICLE NUMBER: 16268

In the format provided by the authors and unedited.

Myeloperoxidase targets oxidative host attacks to *Salmonella* and prevents collateral tissue damage

Nura Schürmann, Pascal Forrer, Olivier Casse, Jiagui Li, Boas Felmy, Anne-Valérie Burgener, Nikolaus Ehrenfeuchter, Wolf-Dietrich Hardt, Mike Recher, Christoph Hess, Astrid Tschan-Plessl, Nina Khanna and Dirk Bumann

Supplementary Information

Table of Contents

Supplementary Note

Computational model parameters

We build a diffusion-reaction model based on a previous neutrophil phagosome model[1] combined with experimental data on *Salmonella* protective enzyme expression as obtained by ex vivo proteomics[2], estimated bacterial ROS production[3,4], adjusted vacuole volume based on electron microscopy[5], and updated reaction kinetics and diffusion constants based on recent reports. Our combined model included four compartments (host cell cytosol, phagosome lumen, *Salmonella* periplasm, *Salmonella* cytosol), 8 small molecules, 10 host and bacterial enzymes, and 27 different reactions including generation and interconversion of various reactive oxygen species (ROS), their diffusion across the phagosomal membrane and the two *Salmonella* membranes, as well as ROS detoxification by *Salmonella* superoxide dismutases, catalases, and peroxidases with quantitative abundance data based on our *ex vivo* proteomics results[13].

Salmonella / phagosome geometry

Salmonella shape was approximated as a cylinder with a length of 2 μM and a diameter of 0.8 μM (ccdb.wishartlab.com/CCDB/intron_new.html). We assumed an outer membrane area of 5.8×10^{-12} m^2, an inner membrane area of 5.4×10^{-12} m^2, a periplasm volume of 5.7×10^{-17} l, and a cytoplasm volume of 8.3×10^{-16} l. The phagosomal membrane was assumed to enclose one single *Salmonella*[5]. The distance between phagosomal membrane and *Salmonella* outer membrane was set to 200 nm based on TEM images[5]. This yielded a phagosomal membrane area of 1.1×10^{-11} m^2, a total phagosome volume of 2.59×10^{-15} l and a phagosome lumen of 1.7×10^{-15} l (excluding the volume occupied by *Salmonella*).

Generation of reactive oxygen species

Salmonella was assumed to endogenously generate $O_2^{\cdot -}$ in periplasm and cytoplasm at rates of 3 μM s^{-1} and 5 μM s^{-1}, respectively[3]; and 10 μM s^{-1} H_2O_2 in the cytoplasm based on a total generation of 14 μM s^{-1} H_2O_2, which included 4 μM s^{-1} due to dismutation of endogenously generated $O_2^{\cdot -}$ [4]. Neutrophil phagosomes were assumed to generate $O_2^{\cdot -}$ at rates of 5.2×10^{-3} mol l^{-1} s^{-1} in the phagosome lumen[1], and to contain 1 mM MPO (normal levels)[1]. Rates for the various reactions of MPO and chloride concentration (100 mM) were used as reported[1].

Membrane permeability for reactive oxygen species

For superoxide in the protonated form $HO_2^{\cdot}$, membrane permeability was set to $9x10^{-6}$ m s^{-1} for all three membranes (phagosomal membrane, *Salmonella* outer and inner membranes)[6], while the deprotonated form was assumed to permeate poorly (< 10^{-9} m s^{-1}) based on reported values for liposomes[6].

For H_2O_2, a membrane permeability of $3.2x10^{-5}$ m s^{-1} was assumed based on the reported permeability of intact *E. coli* ($1.6x10^{-5}$ m s^{-1}; two membranes)[7]. The phagosomal membrane was assumed to have the same permeability based on the range of reported values for mammalian membranes[8].

OCl^- was predicted to have a short reach (33 nm) based on phagosomal protein concentrations[1], reaction rate constants[9], and its diffusion coefficient[10]. This short reach prevented leakage of OCl^- through membranes.

Spontaneous dismutation of superoxide

Superoxide dismutation depends on its protonation state. The total dismutation rate is the sum of rates of two different mechanisms, (i) $HO_2^{\cdot} + O_2^{\cdot -} + H_2O \rightarrow H_2O_2 + O_2 + HO^-$ with a second order rate constant $k_{AB} = 8.5x10^7$ M^{-2} s^{-1}; (ii) $2\ HO_2^{\cdot} \rightarrow H_2O_2 + O_2$, $k_{AA} = 7.6x10^5$ M^{-2} s^{-1}. The relative proportions of $HO_2^{\cdot} + O_2^{\cdot -}$ were calculated based on its pKa of 4.88 [11,12]. We assumed pH 7.4 in the neutrophil phagosome lumen and *Salmonella* periplasm in macrophages.

Detoxification of reactive oxygen species by *Salmonella* enzymes

Absolute *Salmonella* in vivo enzyme copy numbers were obtained from our recent study[13]: SodCI, 39’800 ± 8’300 copies per *Salmonella* cell; SodCII, 370 ± 200; SodA, 4’000 ± 1’000; SodB, 10’200 ± 2’100; KatG, 2’600 ± 500; KatE and KatN, below detection limit; Tpx, 22’000 ± 4’000; AhpC, 15’200 ± 3’500; AhpF, 1’000 ± 400; TsaA, 21’700 ± 3’600.

We used the following kinetic parameters for these enzymes: SodCI, SodCII, $k_{cat}/K_M = 4x10^9$ $M^{-1}s^{-1}$ diffusion-limited[14]; SodA, SodB, $k_{cat}/K_M = 7x10^9$ $M^{-1}s^{-1}$ diffusion-limited[15]; KatG, k_{cat} = 14'000 s^{-1}, K_M = 5.9 mM[16]; Tpx, k_{cat} = 76 s^{-1}, K_M = 1.7 mM[17]; AhpC (and its paralog TsaA), k_{cat} = 55.1 s^{-1}, K_M = 1.4 μM[18]; AhpF, k_{cat} = 25.5 s^{-1}, K_M = 14.3 μM[18]).

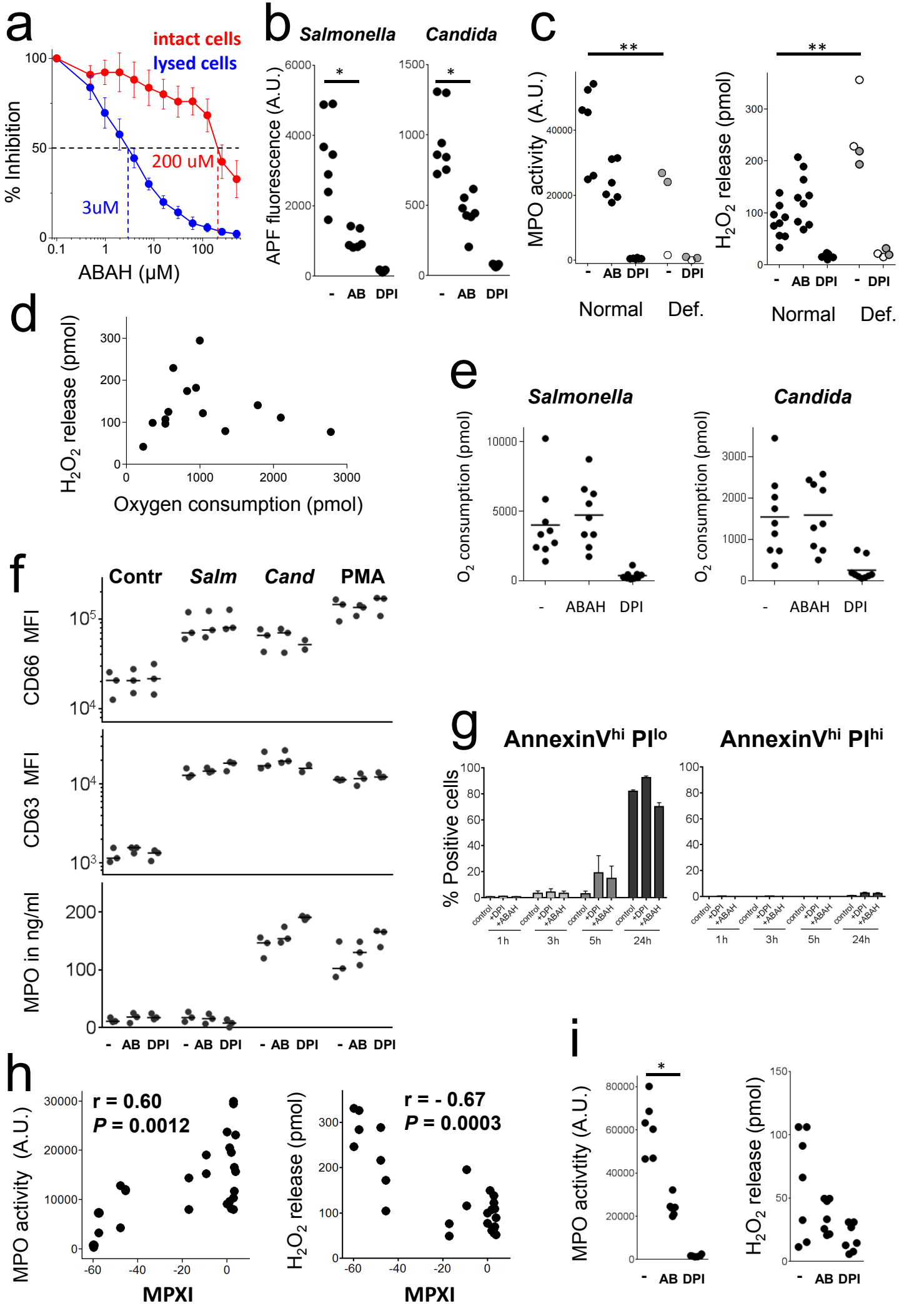
a
intact cells
lysed cells
200 uM
3uM
% Inhibition
ABAH (μM)
b
Salmonella
Candida
APF fluorescence (A.U.)
- AB DPI
c
MPO activity (A.U.)
H2O2 release (pmol)
Normal
Def.
d
H2O2 release (pmol)
Oxygen consumption (pmol)
e
Salmonella
Candida
O2 consumption (pmol)
- ABAH DPI
f
Contr
Salm
Cand
PMA
CD66 MFI
CD63 MFI
MPO in ng/ml
g
AnnexinVhi PIlo
AnnexinVhi PIhi
% Positive cells
control
+DPI
+ABAH
1h
3h
5h
24h
h
r = 0.60
P = 0.0012
r = - 0.67
P = 0.0003
MPO activity (A.U.)
H2O2 release (pmol)
MPXI
i
MPO activity (A.U.)
H2O2 release (pmol)

Supplementary Figure 1: Reactive oxygen species generation and leakage of human neutrophils in vitro.

a, Inhibition of myeloperoxidase activity by ABAH in intact or lysed neutrophils. Data (means and standard deviations of six technical triplicates) from one representative experiment out of two are shown. The dotted lines indicate 50% activity and the corresponding ABAH concentrations for lysed or intact cells, respectively. **b**, MPO activity measured as APF oxidation in neutrophils from seven different normal donors after 60 min stimulation in presence/absence of the MPO inhibitor ABAH (AB) or the NADPH oxidase inhibitor DPI (Wilcoxon test; *, $P< 0.05$). **c**, MPO activity and H_2O_2 release of neutrophils from eight different normal donors (black circles), two partially deficient donors (grey), and two severely deficient donors (empty circles) during stimulation with *Candida* in presence/absence of the MPO inhibitor ABAH (AB) or the NADPH oxidase inhibitor DPI (Kruskal-Wallis multiple comparisons test; **, $P< 0.01$). **d**, Relationship between oxygen consumption and H_2O_2 release in neutrophils stimulated with heat-killed *Candida* for 75 min. Mean values of triplicate wells containing 100'000 neutrophils are shown. **e**, Impact of inhibiting myeloperoxidase with ABAH, or NADPH oxidase with DPI, on oxygen consumption rate after stimulation with heat-killed *Salmonella* and *Candida*. **f**, Impact of inhibitors on neutrophil degranulation. Cells from three different donors were stimulated with PBS (Contr), heat-killed *Salmonella* (*Salm*), *Candida* (*Cand*), or PMA for 75 min in presence/absence of the MPO inhibitor ABAH (AB) or the NADPH oxidase inhibitor DPI. Surface expression of degranulation markers CD63 and CD66 was measured by flow cytometry. MPO release to the extracellular medium was quantified using ELISA. Different stimuli triggered the three degranulation processes to a various degree, but all three assays demonstrated no impact of inhibitors ABAH and DPI on neutrophil degranulation. **g**, Impact of 500 μM ABAH and 10 μM DPI on neutrophil viability. The fraction of cells undergoing apoptosis [annexinV^{hi} propidium iodide $(PI)^{lo}$, left] and cells undergoing necrosis (annexinV^{hi} PI^{hi}, right) at various times after inhibitor addition is shown. Means and standard deviations for four donors measured in one experiment are shown. In all other experiments of this study, cells were exposed to these inhibitors for a maximum of 75 min. **h**, Relationship between donor mean peroxidase index (MPXI) and HOCl generation (left) or H_2O_2 release (right) after stimulation with live or heat-killed *Salmonella* (r, Spearman correlation coefficient). Each dot represents data for an individual human donor. **i**, MPO activity and H_2O_2 release of neutrophils from seven different normal donors during stimulation with 1 nM PMA in presence/absence of the MPO inhibitor ABAH (AB) or the NADPH oxidase inhibitor DPI (Wilcoxon test; *, $P< 0.05$).

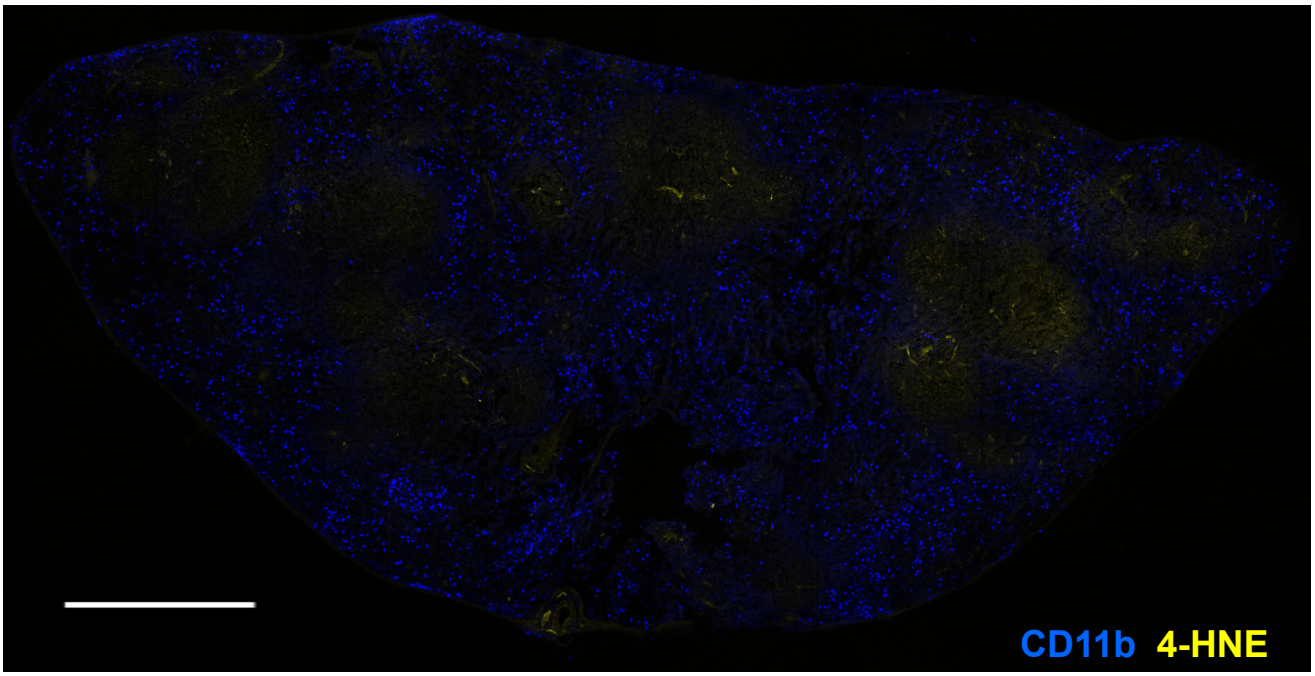

Supplementary Figure 2: Lipid peroxidation in uninfected spleen as detected by an antibody to 4-hydroxynonenal (4-HNE).

Representative micrograph of a spleen cross-section from one out of four uninfected MPO-deficient mice. CD11b^{hi} cells populate the red pulp. 4-HNE signals are undetectable in these areas, whereas some background staining is visible in the white pulp areas (which are negative for CD11b). The scale bar represents 500 μm.

Supplemental References

1 Winterbourn, C. C., Hampton, M. B., Livesey, J. H. & Kettle, A. J. Modeling the reactions of superoxide and myeloperoxidase in the neutrophil phagosome: implications for microbial killing. *J Biol Chem* **281**, 39860-39869 (2006).

2 Burton, N. A. *et al.* Disparate impact of oxidative host defenses determines the fate of Salmonella during systemic infection in mice. *Cell host & microbe* **15**, 72-83, doi:10.1016/j.chom.2013.12.006 (2014).

3 Imlay, J. A. in *EcoSal* (ed R. III.; Kaper Curtiss, J.B.; Squires, C.L.; Karp, P.D.; Neidhardt, F.C.; Slauch, J.M.) Ch. Modul 5.4.4, (ASM Press, 2009).

4 Seaver, L. C. & Imlay, J. A. Are respiratory enzymes the primary sources of intracellular hydrogen peroxide? *J Biol Chem* **279**, 48742-48750 (2004).

5 Beuzon, C. R. *et al.* Salmonella maintains the integrity of its intracellular vacuole through the action of SifA [published erratum appears in EMBO J 2000 Aug 1;19(15):4191]. *EMBO J.* **19**, 3235-3249 (2000).

6 Korshunov, S. S. & Imlay, J. A. A potential role for periplasmic superoxide dismutase in blocking the penetration of external superoxide into the cytosol of Gram-negative bacteria. *Mol Microbiol* **43**, 95-106 (2002).

7 Seaver, L. C. & Imlay, J. A. Hydrogen peroxide fluxes and compartmentalization inside growing Escherichia coli. *J Bacteriol* **183**, 7182-7189 (2001).

8 Makino, N., Sasaki, K., Hashida, K. & Sakakura, Y. A metabolic model describing the H2O2 elimination by mammalian cells including H2O2 permeation through cytoplasmic and peroxisomal membranes: comparison with experimental data. *Biochimica et biophysica acta* **1673**, 149-159, doi:10.1016/j.bbagen.2004.04.011 (2004).

9 Storkey, C., Davies, M. J. & Pattison, D. I. Reevaluation of the rate constants for the reaction of hypochlorous acid (HOCl) with cysteine, methionine, and peptide derivatives using a new competition kinetic approach. *Free radical biology & medicine* **73**, 60-66, doi:10.1016/j.freeradbiomed.2014.04.024 (2014).

10 Kundrat, P., Bauer, G., Jacob, P. & Friedland, W. Mechanistic modelling suggests that the size of preneoplastic lesions is limited by intercellular induction of apoptosis in oncogenically transformed cells. *Carcinogenesis* **33**, 253-259, doi:10.1093/carcin/bgr227 (2012).

11 Behar, D., Czapski, G., Rabani, J., Dorfman, L. M. & Schwarz, H. A. Acid dissociation constant and decay kinetics of the perhydroxyl radical. *The Journal of Physical Chemistry* **74**, 3209-3213, doi:10.1021/j100711a009 (1970).

12 Aurudi, R. L. R., A.B. Reactivity of HO_2/O^{-2} radicals in aqueous solution. *J Phys Chem Ref Data* **14**, 1041–1100 (1985).

13 Steeb, B. *et al.* Parallel exploitation of diverse host nutrients enhances salmonella virulence. *PLoS Pathog* **9**, e1003301 (2013).

14 Stroppolo, M. E. *et al.* Single mutation at the intersubunit interface confers extra efficiency to Cu,Zn superoxide dismutase. *FEBS Lett* **483**, 17-20 (2000).

15 Bull, C. & Fee, J. A. Steady-state kinetic studies of superoxide dismutases: properties of the iron containing protein from Escherichia coli. *Journal of the American Chemical Society* **107**, 3295-3304, doi:10.1021/ja00297a040 (1985).

16 Meir, E. & Yagil, E. Further characterization of the two catalases inEscherichia coli. *Current Microbiology* **12**, 315-319, doi:10.1007/bf01567889 (1985).

17 Baker, L. M. & Poole, L. B. Catalytic mechanism of thiol peroxidase from Escherichia coli. Sulfenic acid formation and overoxidation of essential CYS61. *J Biol Chem* **278**, 9203-9211 (2003).

18 Poole, L. B. Bacterial defenses against oxidants: mechanistic features of cysteine-based peroxidases and their flavoprotein reductases. *Arch Biochem Biophys* **433**, 240-254 (2005).